The Astrophysical Journal, 702:L105–L109, 2009 September 10 doi:10.1088/0004-637X/702/2/L105

CHARACTERIZATION OF CLOUDS IN TITAN'S TROPICAL ATMOSPHERE

Caitlin A. Griffith[1], Paulo Penteado[1], Sebastien Rodriguez[2], Stéphane Le Mouélic[3], Kevin H. Baines[4], Bonnie Buratti[4], Roger Clark[5], Phil Nicholson[6], Ralf Jaumann[7], and Christophe Sotin[4]
[1] Department of Planetary Sciences, University of Arizona, Tucson, AZ 85719, USA
[2] Laboratoire AIM, Université Paris 7/CNRS/CEA-Saclay, DSM/IRFU/SAp, France
[3] Laboratoire de Planétologie et Géodynamique, CNRS, UMR-6112, Université de Nantes, 44000 Nantes, France
[4] Jet Propulsion Laboratory, Pasadena, CA 91109, USA
[5] U.S. Geological Survey, Denver, CO 80225, USA
[6] Department of Astronomy, Cornell University, Ithaca, NY, USA
[7] Institute of Planetary Exploration, Deutsche Zentrum, für Luft- und Raumfahrt, Germany
Received 2009 March 6; accepted 2009 July 31; published 2009 August 19

ABSTRACT

Images of Titan's clouds, possible over the past 10 years, indicate primarily discrete convective methane clouds near the south and north poles and an immense stratiform cloud, likely composed of ethane, around the north pole. Here we present spectral images from Cassini's Visual Mapping Infrared Spectrometer that reveal the increasing presence of clouds in Titan's tropical atmosphere. Radiative transfer analyses indicate similarities between summer polar and tropical methane clouds. Like their southern counterparts, tropical clouds consist of particles exceeding 5 μm. They display discrete structures suggestive of convective cumuli. They prevail at a specific latitude band between 8°–20° S, indicative of a circulation origin and the beginning of a circulation turnover. Yet, unlike the high latitude clouds that often reach 45 km altitude, these discrete tropical clouds, so far, remain capped to altitudes below 26 km. Such low convective clouds are consistent with the highly stable atmospheric conditions measured at the Huygens landing site. Their characteristics suggest that Titan's tropical atmosphere has a dry climate unlike the south polar atmosphere, and despite the numerous washes that carve the tropical landscape.

Key words: convection – methods: analytical – planets and satellites: individual (Titan) – radiative transfer

1. INTRODUCTION

Thick clouds on Titan are sparse, by terrestrial standards, and over the past 10 years, largely confined to high latitudes. In Titan's southern hemisphere, clouds appear near the pole and at −40° latitude (Griffith et al. 1998, 2000; Brown et al. 2002; Roe et al. 2002; Gibbard et al. 2004; Roe et al. 2005; Ádámkovics et al. 2006; Schaller et al. 2006a, 2006b; Hirtzig et al. 2006; Rodriguez et al. 2009). Their hourly temporal evolution, cumuli structures, and positions in the upper troposphere, at ∼25–45 km, indicate that they consist of methane (the second most abundant atmospheric constituent), form through convection, and dissipate through rainfall (Griffith et al. 2000; Porco et al. 2005; Griffith et al. 2005; Turtle et al. 2009). Titan's northern hemisphere displays an increasing number of similarly discrete clouds, hypothesized to result from evaporation (Brown et al. 2009). Yet the major feature is a ∼5400 km stratiform cloud that caps the pole (Griffith et al. 2006). Its lack of cumuli structure and temporal variability and its small ∼3 μm sized particles indicate that it is composed of ethane, a minor atmospheric constituent (Griffith et al. 2006).

General circulation models (GCMs) demonstrate that the winter northern ethane clouds and the summer southern methane clouds result from the circulation (Rannou et al. 2006; Mitchell et al. 2006). Convective methane clouds are explained as triggered by circulation updrafts (Brown et al. 2002; Rannou et al. 2006). Ethane clouds, in contrast, correlate with downdrafts that bring photochemical byproducts (mainly ethane) from the stratosphere to cooler levels near the tropopause where they condense and form stratiform clouds (Griffith et al. 2006; Rannou et al. 2006). At equinox, in 2009 August, the largely pole-to-pole circulation is expected to reverse, thereby inducing a hemisphere swap in polar clouds, with the ethane cloud following winter and the methane cloud following summer (Hourdin et al. 1995; Rannou et al. 2006). A brief Hadley cell circulation may appear near equinox and instigate cloud formation at tropical latitudes (Rannou et al. 2006; Mitchell et al. 2006).

Such seasonal cloud migrations conducted over the 29.5 year period of Titan's orbit are supported by ground-based and Cassini observations, which indicate a greater prevalence of −40° clouds in the past few years compared to polar clouds (Schaller et al. 2006b; Rodriguez et al. 2009). Yet little is known about the rare tropical clouds. Cassini ISS detected a cloud at −14° latitude; its altitude, morphology, and formation were not investigated for lack of spectra (Porco et al. 2005). The Huygens Probe found a tropical cloud over the landing site, at −10° latitude, 193° west longitude, with an optical depth, $\tau \sim 0.001$, too low to discern remotely (Tomasko et al. 2005).

2. OBSERVATIONS

We have detected the presence of five tropical clouds in the spectral images recorded by Cassini's Visual and Infrared Mapping Spectrometer (VIMS) during the spacecraft's nominal mission of 44 flybys (Figures 1 and 2) from 2004 July 3 to 2008 May 28. Each IR pixel in the VIMS images of the clouds consists of a 0.88–5.1 μm spectrum with a bandpass of 16.6 nm (Brown et al. 2004). Within the wavelength region that we analyze, 1–1.6 μm, the spectrum is defined by absorption due to methane vibrational bands and scattering from haze and methane cloud particulates. Titan's clouds are identified by albedo enhancements at wavelengths between the methane bands where the atmosphere is most transparent. In the center of these "window" wavelengths (e.g., 1.08, 1.28, and 1.58 μm) the surface is sampled; yet in the wings of these windows there exist wavelengths that probe the troposphere above ∼12 km, but not the surface (Griffith et al. 1998) (Figure 3). From the analysis of these wavelengths, a survey of VIMS data also detected one of

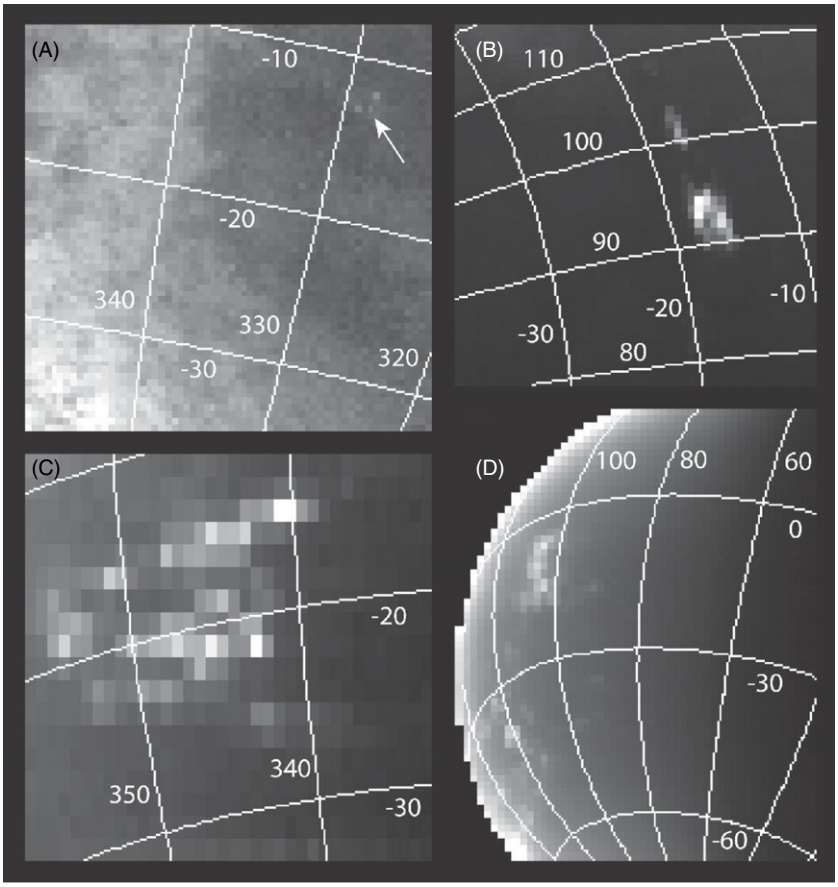

Figure 1. Tropical clouds were detected on Titan flybys T17 (panel A), T21 (C), T43 (B) and T 44 (D), in VIMS cubes V1536359596, V1544636893, V1589259395, and V1590646944, respectively. The T17 cloud can only be seen at wavelengths that probe down to the surface; it is indicated by the relatively bright pixels (arrow) over dark surface terrain at 2.8 μm wavelength (A). The other clouds (B–D) are shown at 2.9 μm, where the surface reflected radiation is insignificant.

Table 1
Tropical Clouds

Flyby & Date	θ_{ph}	Lat	Z (km)	τ
T17 2006 Sep 7	55°	10°S	~12	< 0.1
T21 2006 Dec 12	68°	17°S	18 ± 3	0.3
T29 2007 Apr 26	37°	9°S	12 ± 3	0.1
T43 2008 May 12	103°	10°S	~24	0.6
T44 2008 May 28	93°	17°S	16 ± 4	8.0

the clouds, that from flyby T21 (Rodriguez et al. 2009), which is analyzed in detail here. The low T17 and T29 clouds were difficult to distinguish spectroscopically from the surface. Thus the T29 cloud's temporal variations disclosed its presence. It was seen on 2007 April 26, yet did not exist on 2007 April 10 (Figure 2) and had vanished by 2007 June 29. The T17 cloud was inferred from its relatively high enhancement at 2.8 μm. The other three tropical clouds were high enough to cause a distinct brightening at wavelengths that do not significantly probe the surface (Figure 1).

3. CLOUD CHARACTERISTICS

To determine the clouds' altitudes and thicknesses we approximate the radiative transfer equation with discrete ordinates calculations, following previous work (Griffith et al. 2005, 1991), with the exception that we use 32 streams (Stamnes et al. 1988), which is necessary to accurately characterize the haze's highly peaked phase function (Tomasko et al. 2008b). To quantify the cloud altitudes, we vertically sample the atmosphere with 70 layers that extend from the surface to 375 km altitude. Our analysis is limited to the 1.0–1.6 μm spectrum, where methane absorption properties and the haze phase function, single scattering albedo, and density profile have been measured in situ by the Huygens Descent Imager/Spectral Radiometer (DISR) (Tomasko et al. 2008a, 2008b). These values, determined at -10° latitude, apply to the nearby latitudes studied here, because KECK and VIMS spectra indicate constant methane and haze characteristics between -5° and -15° latitude. In addition, Titan's thermodynamics point to a constant methane abundance at tropical latitudes (Griffith et al. 2008). Thus the haze and methane characteristics measured by Huygens and used in our calculations (Fulchignoni et al. 2005; Niemann et al. 2005; Tomasko et al. 2008a, 2008b) match the conditions sampled by the data studied here. The only free parameters in our calculations are the surface albedo, cloud optical depth, and cloud height.

The three unknown quantities are derived from three measured variables. The most transparent sections in the windows probe the surface albedo. The wavelengths that define the wings of the methane bands, and thus the windows, each sample a different tropospheric altitude range (Figure 3). Thus the slope of the wings of the windows coupled with the albedo at some intermediate point within the wings indicate both the cloud's optical depth and height. Figure 4 shows how the cloud's altitude affects the spectra of a low and tenuous cloud and a higher and thicker cloud. In this figure, spectra of cloudy regions are subtracted from cloud-free spectra to bring out the more subtle

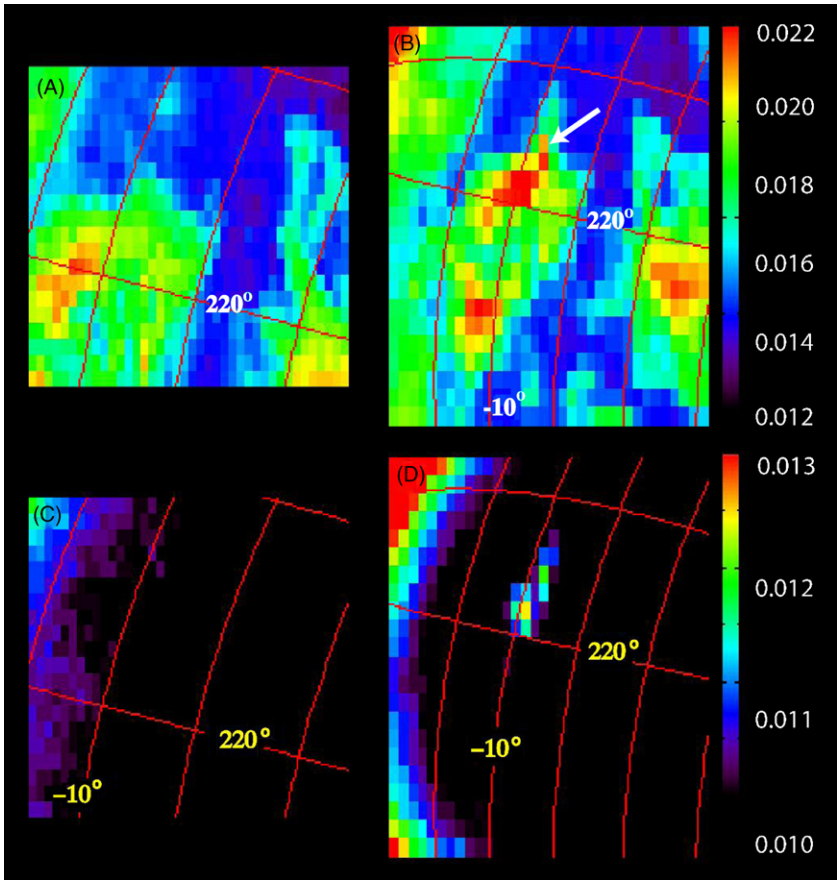

Figure 2. Clouds appear at ∼9° S latitude and ∼225° longitude on 2007 April 26, during the T29 flyby (panels B and D), in the VIMS cube V1556356726, but not on 2007 April 10, during the T28 flyby (A and C), in the VIMS cube V1554960431. Titan's 2.8 μm albedo (A and B) exhibits the surface albedo as well as the clouds' signature, above the 220° longitude line and north (right) of −10° latitude, as shown by the arrow. At 2.9 μm (C and D), the atmospheric methane opacity limits visibility to the surface, and albedo variations are caused by limb brightening (left edges) and (in D) the clouds. Spacings of latitude and west longitude grid lines are 10° and 20°, respectively.

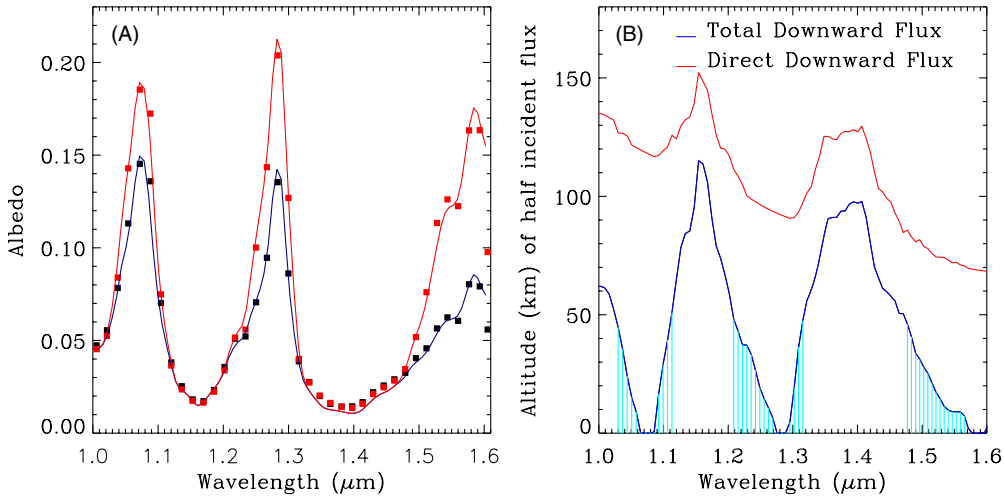

Figure 3. Panel A: spectra of the tropical cloud observed during Cassini's T44 flyby, pixel [33, 24] from cube V1590646944 (red squares), and of the cloud-free atmosphere, pixel [33, 21] (black squares) are compared to calculated spectra of a clear atmosphere and one with a cloud at 19 km altitude (solid black and red lines). Panel B: altitudes where half the incident direct (red) and direct + diffuse (blue) downward fluxes are extinguished, assuming the scattering angles of the T21 cloud. Scattering by haze attenuates the direct flux in the stratosphere (red) such that primarily diffuse light samples the troposphere at narrow wavelength regions (cyan lines).

effects of the clouds. Comparisons between calculated and observed spectra are used to derive the highest altitudes, Z (km), and greatest optical depths of the clouds, τ, assuming full cloud coverage within the pixel. These results are given in Table 1, along with the phase angles, θ_{ph}, of the observations.

Examples of the derivations of the cloud altitudes are shown in Figure 4. As indicated in panels B and D, the calculations do not precisely match data. This mismatch occurs as a result of several sources of uncertainties. Noise contributes ∼1% of the signal; uncertainties due to methane and haze provide an

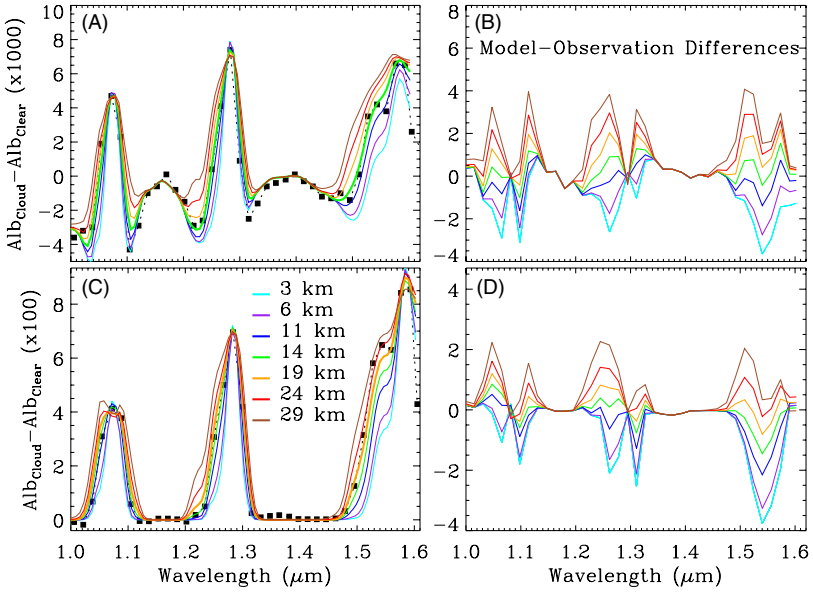

Figure 4. Panel A: a spectrum of the T29 cloud, pixel [15, 09] from the V1556356726 observation, subtracted by a spectrum recorded 16 days prior (pixel [12, 11] of the T28 V1554960431) of the same location when cloudless (black squares). Models of the cloud to cloudless spectral difference are shown for clouds at several indicated altitudes. Cloud models assume 5 μm sized spherical particles. A column abundance of 150,000 cm^{-2} is derived from the peaks of the differences between the spectra. The different observing angles of the measurements cause a negative value in the spectral regions (e.g., at 1.10–1.24 μm) that sample the stratosphere. Panel C: difference of cloudy and clear atmosphere spectra from the T44 flyby (shown in Figure 3) are compared to the difference of calculated cloudy and clear atmosphere spectra. Cloud models assume a column of 5.5 $\times$ 10^6 cm^{-2} particles of radius 5 μm, which establish the peaks of the differences. Panels B and D: differences, or "contrasts," between the measured cloud and cloud-free difference and the calculated difference shown in panels A and C, using the same color designations. The contrasts of the 11 km cloud and 14 km cloud models agree to within 15% of the measured cloud to cloud-free spectral difference shown in panel A, and thus provide viable fits to the data. The contrasts for 14 km cloud and 19 km cloud models agree to within 15% of the measured difference shown in panel C, and thus fit the data.

estimated error in the calculated difference between the spectra of ~6% each. This error has been estimated by comparing the fits of VIMS spectra that sample the same Titan latitude over a range of lighting angles and surface albedos. Thus two models whose difference match the difference in the observations (e.g., panels A and C in Figure 4) to within 15% (panels B and D, Figure 4) are considered a viable fit to the data. We find, in addition, that the clouds exhibit the same optical depth at 2 μm and 5 μm, indicating a radius of at least 5 μm, assuming spherical particles, characteristic of liquid drops. An upper limit on the particle size of the T29 cloud of ~30 μm is indicated by its invariance over 7.3 hr. During this time period a particle of this size would have evaporated Graves et al. (2008) or fallen to the surface based on the fall times calculated by Barth & Toon (2003).

We find no particular commonality in the surface features over which the tropical clouds reside. The T21 cloud sits over dunes, while the T43 and T44 clouds appear over RADAR and near-IR bright terrain. The T29 clouds occur near small dark (and therefore smooth) areas of ~5 km diameter at [−9°, 224°]; but these "plains" are common, with ~8 in the nearby 200 × 200 km^2 region. The [−7°, 230°] position is contained within a dark terrain of ~37 km in diameter. The spatial resolution is insufficient to discern the geology.

Titan's tropical clouds range in thickness and vary daily, similar to the more ubiquitous southern clouds. Other resemblances are their methane composition and their sizes, which extend from one hundred to one thousand kilometers, with tails that follow longitude lines, suggesting transport by zonal winds. Tropical clouds prevail at the particular latitude band of 8°–20°, suggesting that, analogous to south polar clouds, the general circulation affects their origins. Nonetheless, they differ fundamentally from the southern clouds; they are confined to lower altitudes.

4. DISCUSSION

The altitudes of clouds, if convective, provide an indication of the stability and humidity profile of the troposphere. Titan's atmosphere above 15 km is statically stable; thus convection initiates below this level. The altitude reached by plumes depends on their buoyancy, i.e. the temperature of the rising parcel, which depends on the release of latent heat, and therefore the original methane content of the parcel. Although there are no measurements of Titan's humidity at high latitudes, the clouds indicate a surface humidity exceeding 60%, without which, parcels lack the latent heat needed to power convection up the tropopause (~45 km) where they are detected (Hueso & Sánchez-Lavega 2006; Barth & Rafkin 2007; Griffith et al. 2008). Measurements better characterize the tropical atmosphere. The Huygens probe determined methane abundance and temperature profiles at −10° latitude and 191° W longitude (Niemann et al. 2005; Fulchignoni et al. 2005). This unique methane humidity profile, with a 45% value at the surface (Tokano et al. 2006), allows convective updrafts to reach ~26 km altitude (Griffith et al. 2008). Yet, without a change in the methane mixing ratio below 7 km altitude, convection remains weak and confined below 26 km (Griffith et al. 2008). These quiescent conditions do not obviously lead to the formation of the rainstorms that carved tropical washes and dry lake beds, such as those that surround the probe landing site (Griffith et al. 2008).

The several processes that might conceivably humidify the lower troposphere sufficiently to form high convective clouds are not indicated by present measurements of Titan's tropics. Unlike Earth, Titan's weather is weakly powered, with only 1% of the incident solar radiation available for sensible heat and surface evaporation (McKay et al. 1989). This flux increases the humidity of the tropical tropopause by, on

average, only 2% over the course of Titan's summer (Griffith et al. 2008). Small-scale wind-powered evaporation destabilizes the boundary layer on Earth and is hypothesized to explain the high northern latitude clouds on Titan (Brown et al. 2009). Yet the lack of surface liquids and the high stability of the tropical atmosphere argues that such small-scale events will not extend up to the level of free convection at 9 km in the tropical atmosphere, as needed to drive convective clouds up to the tropopause. Unlike Earth, Titan's condensable resides mainly in the atmosphere, ∼5 m (Tokano et al. 2006), rather than on the surface, ∼1 m, (Lorenz et al. 2008); thus in theory, a vertical redistribution of the abundant methane vapor could destabilize the atmosphere. Seasonal cooling above 25 km of 2 K is sufficient to condense and transport, through precipitation, enough methane to saturate the atmosphere at 4–9 km (Griffith et al. 2008). Vertical perturbations of a saturated atmosphere at 4 km would cause parcels to rise to the upper troposphere. Nonetheless, such a tropopause source of methane is not indicated by the methane abundance at the landing site, which is highest at the surface. It is also not clear whether temperatures change by 2 K above 25 km in the tropics. Such a possibility will be tested with Cassini Radio measurements. Cryo-volcanism can also increase the humidity; yet evidence for volcanic activity does not appear in RADAR images of the cloudy regions. Thus the low insolation, apparent lack of surface liquids and volcanism, and the atmospheric stability suggest that the moon's tropical humidity remains largely unchanged in the current climate (Griffith et al. 2008).

The increased presence of tropical clouds as well as their preference for the southern latitude band between -8° and -20° latitude suggest that their formation is triggered by an overturning of Titan's circulation, which will continue to cloud the tropical skies for several years. While stratiform clouds can form in the upper troposphere from temperature and pressure perturbations, convective clouds must form below ∼26 km to be consistent with the conditions measured by the Huygens probe. So far the tropical clouds that are discrete and short, thus likely convective, reside below 26 km. Consistent with the thermodynamics of Titan's probe site (Griffith et al. 2008), no increase in humidity is indicated. Future observations will determine whether convective tropical clouds remain below 26 km as their prevalence increases and subsides with the seasons. High convective clouds might point to a vertical redistribution of methane vapor or volcanism. Continued low clouds would indicate a dry tropical climate, in contrast to the variable polar climate with its summer storms.

C.A.G.'s research is funded by NASA's Cassini Program. P.P.'s work is supported by the Brazilian Governments CAPES scholarship and NASA's Cassini Program.

REFERENCES

Ádámkovics, M., de Pater, I., Hartung, M., Eisenhauer, F., Genzel, R., & Griffith, C. A. 2006, J. Geophys. Res. (Planets), 111, 7
Barth, E. L., & Rafkin, S. C. R. 2007, Geophys. Res. Lett., 34, 3203
Barth, E. L., & Toon, O. B. 2003, Icarus, 162, 94
Brown, M. E., Bouchez, A. H., & Griffith, C. A. 2002, Nature, 420, 795
Brown, M. E., Schaller, E. L., Roe, H. G., Chen, C., Roberts, J., Brown, R. H., Baines, K. H., & Clark, R. N. 2009, Geophys. Res. Lett., 36, 1103
Brown, R. H., et al. 2004, Space Sci. Rev., 115, 111
Fulchignoni, M., et al. 2005, Nature, 438, 785
Gibbard, S. G., et al. 2004, Icarus, 169, 429
Graves, S. D. B., McKay, C. P., Griffith, C. A., Ferri, F., & Fulchignoni, M. 2008, Planet. Space Sci., 56, 346
Griffith, C., Hall, J. L., & Geballe, T. R. 2000, Science, 290, 509
Griffith, C. A., McKay, C. P., & Ferri, F. 2008, ApJ, 687, L41
Griffith, C. A., Owen, T., Miller, G., & Geballe, T. 1998, Nature, 395, 575
Griffith, C. A., Owen, T., & Wagener, R. 1991, Icarus, 93, 362
Griffith, C. A., et al. 2005, Science, 310, 474
Griffith, C. A., et al. 2006, Science, 313, 1620
Hirtzig, M., et al. 2006, A&A, 456, 761
Hourdin, F., Talagrand, O., Sadourny, R., Courtin, R., Gautier, D., & McKay, C. P. 1995, Icarus, 117, 358
Hueso, R., & Sánchez-Lavega, A. 2006, Nature, 442, 428
Lorenz, R. D., et al. 2008, Geophys. Res. Lett., 35, 2206
McKay, C. P., Pollack, J. B., & Courtin, R. 1989, Icarus, 80, 23
Mitchell, J. L., Pierrehumbert, R. T., Frierson, D. M. W., Caballero, R., Ferri, F., Fulchignoni, M., & Niemann, H. B. 2006, Proc. Natl Acad. Sci, 103, 18421
Niemann, H. B., et al. 2005, Nature, 438, 779
Porco, C. C., et al. 2005, Nature, 434, 159
Rannou, P., Montmessin, F., Hourdin, F., & Lebonnois, S. 2006, Science, 311, 201
Rodriguez, S., et al. 2009, Nature, 459, 678
Roe, H. G., Bouchez, A. H., Trujillo, C. A., Schaller, E. L., & Brown, M. E. 2005, ApJ, 618, L49
Roe, H. G., de Pater, I., Macintosh, B. A., & McKay, C. P. 2002, ApJ, 581, 1399
Schaller, E. L., Brown, M. E., Roe, H. G., & Bouchez, A. H. 2006a, Icarus, 182, 224
Schaller, E. L., Brown, M. E., Roe, H. G., Bouchez, A. H., & Trujillo, C. A. 2006b, Icarus, 184, 517
Stamnes, K., Tsay, S.-C., Jayaweera, K., & Wiscombe, W. 1988, Appl. Opt., 27, 2502
Tokano, T., McKay, C. P., Neubauer, F. M., Atreya, S. K., Ferri, F., Fulchignoni, M., & Niemann, H. B. 2006, Nature, 442, 432
Tomasko, M. G., Bézard, B., Doose, L., Engel, S., & Karkoschka, E. 2008a, Planet. Space Sci., 56, 624
Tomasko, M. G., Doose, L., Engel, S., Dafoe, L. E., West, R., Lemmon, M., Karkoschka, E., & See, C. 2008b, Planet. Space Sci., 56, 669
Tomasko, M. G., et al. 2005, Nature, 438, 765
Turtle, E. P., Perry, J. E., McEwen, A. S., DelGenio, A. D., Barbara, J., West, R. A., Dawson, D. D., & Porco, C. C. 2009, Geophys. Res. Lett., 36, 2204